

Effect of Fermi-liquid interactions on the low temperature de Haas–van Alphen oscillations in quasi-two-dimensional conductors

This article has been downloaded from IOPscience. Please scroll down to see the full text article.

2008 J. Phys.: Condens. Matter 20 155105

(<http://iopscience.iop.org/0953-8984/20/15/155105>)

View [the table of contents for this issue](#), or go to the [journal homepage](#) for more

Download details:

IP Address: 129.252.86.83

The article was downloaded on 29/05/2010 at 11:28

Please note that [terms and conditions apply](#).

Effect of Fermi-liquid interactions on the low temperature de Haas–van Alphen oscillations in quasi-two-dimensional conductors

Natalya A Zimbovskaya

Department of Physics and Electronics, University of Puerto Rico-Humacao, CUH Station, Humacao, PR 00791, USA

and

Institute for Functional Nanomaterials, University of Puerto Rico, San Juan, PR 00931, USA

Received 17 December 2007, in final form 6 February 2008

Published 10 March 2008

Online at stacks.iop.org/JPhysCM/20/155105

Abstract

In this work we present the results of theoretical analysis of the de Haas–van Alphen oscillations in quasi-two-dimensional conductors. We have been studying the effect of the Fermi-liquid correlations of charge carriers on the above oscillations. It was shown that at reasonably low temperatures and weak electron scattering the Fermi-liquid interactions may cause noticeable changes in both amplitude and shape of the oscillations even at realistically small values of the Fermi-liquid parameters. Also, we show that the Fermi-liquid interactions in the system of the charge carriers may cause magnetic instability of a quasi-two-dimensional conductor near the peaks of quantum oscillations in the electron density of states at the Fermi surface, indicating the possibility for the diamagnetic phase transition within the relevant ranges of the applied magnetic fields.

(Some figures in this article are in colour only in the electronic version)

1. Introduction

Magnetic quantum oscillations [1–3] have been recognized as one of the major tools to map Fermi surfaces (FSs) in metals. Analysis of the experimental data is now a well established procedure and is based on the classical paper by Lifshitz and Kosevich (LK) [4], who first laid out a quantitative theory of the de Haas–van Alphen effect. The LK expression for the oscillating part of the thermodynamic potential and magnetization of metallic electrons in a strong (quantizing) magnetic field \mathbf{B} was derived assuming that conduction electrons are noninteracting quasiparticles in a periodic crystal potential. This potential determines the electron dispersion, $E(\mathbf{p})$ (\mathbf{p} being the electron quasimomentum), and therefore the effective mass of conduction electrons m^* and their FS. In fact, conduction electrons interact with each other. Studies of modifications of the LK results arising due to electron–electron interactions within the general many-body quantum field-theoretical approach started in the early 1960s in the works of Luttinger [5], and continued through the next three decades [6]. It was shown that electron–electron interactions

may bring noticeable changes in the de Haas–van Alphen oscillations, which makes further analysis worthwhile.

One of the oldest and still powerful methods to deal with electron–electron interaction is the Landau Fermi-liquid (FL) theory [7–9]. It is important to realize that while the *phenomenological* Fermi-liquid theory and the microscopic many-body perturbation theory (and, when applicable, the exact density functional theory) by definition lead to the same observable quantities, such as response to an external field, both the zero approximation and its renormalization depend on the approach taken. A discussion to this effect in application to the dielectric response of metals can be found, for instance, in [10]. It is always instructive to look at the same phenomenon from different points of view. Respecting the value of the many-body perturbation theory as applied to quantum oscillations [6], we emphasize that the Fermi-liquid theory has provided important insights in such areas, relevant for the de Haas–van Alphen physics, as high frequency collective modes in metals [11–16], or oscillations of various thermodynamic observables in quantizing magnetic fields [17–20].

An advantage of this phenomenological theory is that it enables us to describe the effects of quasiparticle interactions in a way that makes the interpretation of the results rather transparent, as compared with the field-theoretical methods. At the same time the many-body approach brings general but cumbersome results, and usually it takes great calculational efforts and/or significant simplifications to get suitable expressions for comparison with experimental data. What is more important, adopted simplifications may lead to omission of some qualitative effects of electron–electron interactions in quantum oscillations, as we show below.

In the last two decades an entire series of quasi-two-dimensional (Q2D) materials with metallic type conductivity has been synthesized. These are organic conductors belonging to the family of tetrathiafulvalene salts, dichalcogenides of transition metals, intercalated compounds and some others. At present, these materials attract a significant interest. Their electronic properties are intensively studied, and the de Haas–van Alphen effect is employed as a tool in these studies [2, 3]. Correspondingly, the theory of this effect in the Q2D materials is currently being developed [21–26]. The present analysis of the effect of Fermi-liquid interactions on the de Haas–van Alphen oscillations contributes to the above theory. Also, the analysis is motivated by the special features in the electron spectra in Q2D materials providing better opportunities for the Fermi-liquid effects to be manifested, as was mentioned in some earlier works [17, 20].

In this paper we show how renormalizations of conduction electron characteristics arising from FL interactions affect quantum oscillations, and we express them in the form appropriate for comparison with experiments. Also, we show that a magnetic phase transition leading to emergence of diamagnetic domains may happen at low temperatures when the cyclotron quantum $\hbar\omega$ is very large compared to the temperature expressed in the energy units: ($\hbar\omega \gg k_B T$). We emphasize that the analyzed effects are different from the many-body renormalizations of the band structure. Within the phenomenological theory the latter are already included in the ground state of conduction electrons.

2. Fermi-liquid renormalizations of the conduction electron characteristics

Within the phenomenological Landau FL theory single quasiparticle energies are renormalized, and the renormalization is determined by the distribution of excited quasiparticles. Accordingly, the energy of a ‘bare’ (noninteracting) quasiparticle $E_0(\mathbf{p})$ moving in the effective crystal potential is replaced by the renormalized energy defined by the relation [7]

$$E_\sigma(\mathbf{p}, \mathbf{r}, t) = E_0(\mathbf{p}) + \sum_{\mathbf{p}'\sigma'} F(\mathbf{p}, \mathbf{s}; \mathbf{p}', \mathbf{s}') \delta\rho(\mathbf{p}', \mathbf{s}', \mathbf{r}, t). \quad (1)$$

Note that $E_0(\mathbf{p})$ here is the energy spectrum in the absence of any excited quasiparticles, that is, at equilibrium and at zero temperature, while $\delta\rho(\mathbf{p}', \mathbf{s}', \mathbf{r}, t)$ represents the nonequilibrium part of the electron distribution function, which may depend on both position \mathbf{r} of the quasiparticle

and time t . Also, \mathbf{s}, \mathbf{s}' are spin Pauli matrices (σ is the spin quantum number), and $F(\mathbf{p}, \mathbf{s}; \mathbf{p}', \mathbf{s}')$ is the Fermi-liquid kernel (Landau correlation function), which describes additional renormalization of the quasiparticle spectrum due to interaction with other excited quasiparticles (but not with all electrons in the system, which is included in $E_0(\mathbf{p})$). Neglecting spin–orbit interactions, the Landau correlation function may be written as

$$F(\mathbf{p}, \mathbf{s}; \mathbf{p}', \mathbf{s}') = \varphi(\mathbf{p}, \mathbf{p}') + 4\psi(\mathbf{p}, \mathbf{p}')(\mathbf{s}\mathbf{s}'). \quad (2)$$

As follows from equation (1), the conduction electron velocity $\mathbf{v} = \nabla_{\mathbf{p}} E$ differs from the bare velocity $\mathbf{v}_0 = \nabla_{\mathbf{p}} E_0$. To proceed in our analysis we need to bring velocities \mathbf{v} and \mathbf{v}_0 into correlation. For brevity we do not explicitly write out the variables \mathbf{r}, t in equation (1) in further calculations. This omission does not influence the results. Differentiating equation (1) we obtain

$$\mathbf{v}_\sigma(\mathbf{p}) = \mathbf{v}_0(\mathbf{p}) + \nabla_{\mathbf{p}} \left[\sum_{\mathbf{p}'\sigma'} F(\mathbf{p}, \mathbf{s}; \mathbf{p}', \mathbf{s}') \delta\rho(\mathbf{p}', \mathbf{s}') \right]. \quad (3)$$

The electron distribution function $\rho(\mathbf{p}, \mathbf{s})$ is the sum of the equilibrium part ρ_0 (the latter coincides with the Fermi distribution function for quasiparticles with single particle energies $E_0(\mathbf{p})$) and the nonequilibrium correction $\delta\rho$. Multiplying both parts of equation (3) by $\rho(\mathbf{p}, \mathbf{s})$ and performing summation over \mathbf{p}, σ we get

$$\sum_{\mathbf{p}\sigma} \rho(\mathbf{p}, \mathbf{s}) \mathbf{v}_\sigma(\mathbf{p}) = \sum_{\mathbf{p}\sigma} \rho(\mathbf{p}, \mathbf{s}) \mathbf{v}_0(\mathbf{p}) + \sum_{\mathbf{p}\sigma} \rho(\mathbf{p}, \mathbf{s}) \nabla_{\mathbf{p}} \times \left[\sum_{\mathbf{p}'\sigma'} F(\mathbf{p}, \mathbf{s}; \mathbf{p}', \mathbf{s}') \delta\rho(\mathbf{p}', \mathbf{s}') \right]. \quad (4)$$

The second term on the right-hand side of equation (4) could be converted to the form

$$- \sum_{\mathbf{p}\sigma} \left[\sum_{\mathbf{p}'\sigma'} F(\mathbf{p}, \mathbf{s}; \mathbf{p}', \mathbf{s}') \delta\rho(\mathbf{p}', \mathbf{s}') \right] \nabla_{\mathbf{p}} \rho(\mathbf{p}, \mathbf{s}). \quad (5)$$

Keeping only the terms linear in $\delta\rho$ (which is supposed to be small compared to the equilibrium part of the distribution function), we may approximate $\nabla_{\mathbf{p}} \rho$ as $\mathbf{v}_\sigma(\mathbf{p}) \frac{\partial f_{\mathbf{p}\sigma}}{\partial E_{\mathbf{p}\sigma}}$. Here, f is the Fermi distribution function and the quasiparticle energies $E_\sigma(\mathbf{p})$ correspond to the local equilibrium of the electron liquid. Also, assuming that the FS of a considered metal possesses a center of symmetry, we get

$$\begin{aligned} \sum_{\mathbf{p}\sigma} \rho(\mathbf{p}, \mathbf{s}) \mathbf{v}_\sigma(\mathbf{p}) &= \sum_{\mathbf{p}\sigma} \delta\rho(\mathbf{p}, \mathbf{s}) \mathbf{v}_\sigma(\mathbf{p}), \\ \sum_{\mathbf{p}\sigma} \rho(\mathbf{p}, \mathbf{s}) \mathbf{v}_0(\mathbf{p}) &= \sum_{\mathbf{p}\sigma} \delta\rho(\mathbf{p}, \mathbf{s}) \mathbf{v}_0(\mathbf{p}). \end{aligned} \quad (6)$$

Then, using the well known relation $F(\mathbf{p}, \mathbf{s}; \mathbf{p}', \mathbf{s}') = F(\mathbf{p}', \mathbf{s}'; \mathbf{p}, \mathbf{s})$ and carrying out the replacement $\mathbf{p}, \mathbf{s} \rightleftharpoons \mathbf{p}', \mathbf{s}'$

in the sums included in equation (5), we could rewrite equation (4) as

$$\begin{aligned} & \sum_{\mathbf{p}\sigma} \delta\rho(\mathbf{p}, \mathbf{s}) \left[\mathbf{v}_\sigma(\mathbf{p}) + \sum_{\mathbf{p}'\sigma'} \frac{\partial f_{\mathbf{p}'\sigma'}}{\partial E_{\mathbf{p}'\sigma'}} F(\mathbf{p}, \mathbf{s}; \mathbf{p}', \mathbf{s}') \mathbf{v}_{\sigma'}(\mathbf{p}') \right] \\ & = \sum_{\mathbf{p}\sigma} \delta\rho(\mathbf{p}, \mathbf{s}) \mathbf{v}_0(\mathbf{p}). \end{aligned} \quad (7)$$

Solving this for \mathbf{v} , we obtain

$$\mathbf{v}_\sigma(\mathbf{p}) = \mathbf{v}_0(\mathbf{p}) - \sum_{\mathbf{p}', \sigma'} \frac{\partial f_{\mathbf{p}'\sigma'}}{\partial E_{\mathbf{p}'\sigma'}} F(\mathbf{p}, \mathbf{s}; \mathbf{p}', \mathbf{s}') \mathbf{v}_{\sigma'}(\mathbf{p}'). \quad (8)$$

Exact expressions for the functions $\varphi(\mathbf{p}, \mathbf{p}')$ and $\psi(\mathbf{p}, \mathbf{p}')$ are of course unknown. The simplest approximation is to treat them as constants. This approximation is reasonable as long as the interaction of quasiparticles (located at \mathbf{r} and \mathbf{r}' , respectively) is extremely short range, so that the interaction can be approximated as $V(\mathbf{r}, \mathbf{r}') = I\delta(\mathbf{r} - \mathbf{r}')$. Using this approximation one captures some FL effects but in the general case it is not sufficient.

As a next step, one may expand the Fermi-liquid functions in the equation (2) in basis functions respecting the crystal symmetry, such as Allen's Fermi surface harmonics [27]:

$$\begin{aligned} \varphi(\mathbf{p}, \mathbf{p}') &= \sum_{j=1}^d \sum_{m=1}^{d_j} \varphi_j(p, p') R_{jm}(\theta, \Phi) R_{jm}^*(\theta', \Phi'), \\ \psi(\mathbf{p}, \mathbf{p}') &= \sum_{j=1}^d \sum_{m=1}^{d_j} \psi_j(p, p') R_{jm}(\theta, \Phi) R_{jm}^*(\theta', \Phi'). \end{aligned} \quad (9)$$

Here, we introduce spherical coordinates for \mathbf{p} : $\mathbf{p} = (p, \theta, \Phi)$; d is the order of the point group; index j labels irreducible representations of the group; d_j is the dimension of the j th irreducible representation; $\{R_{jm}(\theta, \Phi)\}$ is a basis of the j th irreducible representation including d_j functions.

For an isotropic metal the spherical harmonics Y_{jm} can be used as the basis. Including orbital moments up to $j = 2$ we have, for a cubic symmetry (cubic harmonics),

$$\begin{aligned} \begin{pmatrix} \varphi(\mathbf{p}, \mathbf{p}') \\ \psi(\mathbf{p}, \mathbf{p}') \end{pmatrix} &= \begin{pmatrix} \varphi_0 \\ \psi_0 \end{pmatrix} + \begin{pmatrix} \varphi_1 \\ \psi_1 \end{pmatrix} (p_x p'_x + p_y p'_y + p_z p'_z) \\ &+ \begin{pmatrix} \varphi_{21} \\ \psi_{21} \end{pmatrix} (p_z p'_z p_x p'_x + p_z p'_z p_y p'_y + p_x p'_x p_y p'_y) \\ &+ \begin{pmatrix} \varphi_{22} \\ \psi_{22} \end{pmatrix} (p_x^2 - p_y^2)(p_x'^2 - p_y'^2) \\ &+ \frac{1}{3} \begin{pmatrix} \varphi_{22} \\ \psi_{22} \end{pmatrix} (2p_z^2 - p_x^2 - p_y^2)(2p_z'^2 - p_x'^2 - p_y'^2). \end{aligned} \quad (10)$$

The coefficients φ, ψ are material dependent constants. A common feature of Q2D metals is their layered structure with a pronounced anisotropy of the electrical conductivity. In such materials electron energy only weakly depends on the quasimomentum projection $p = \mathbf{p}\mathbf{n}$ on the normal \mathbf{n} to the layer plane. In further consideration we assume $\mathbf{n} = (0, 0, 1)$ and we neglect the asymmetries of the electron spectrum in the layer planes. Then the relevant Fermi surface is axially symmetrical.

For systems with an axial symmetry this expression (10) needs to be correspondingly modified. For instance, in the first order we have

$$\begin{aligned} \begin{pmatrix} \varphi(\mathbf{p}, \mathbf{p}') \\ \psi(\mathbf{p}, \mathbf{p}') \end{pmatrix} &= \begin{pmatrix} \varphi_0 \\ \psi_0 \end{pmatrix} + \begin{pmatrix} \varphi_{10} \\ \psi_{10} \end{pmatrix} p_z p'_z \\ &+ \begin{pmatrix} \varphi_{11} \\ \psi_{11} \end{pmatrix} (p_x p'_x + p_y p'_y). \end{aligned} \quad (11)$$

This expression will be used from now on in the present paper.

When an external magnetic field $\mathbf{B} = (0, 0, B)$ is applied the spin degeneracy of the single electron energies is lifted, and we can write

$$E_{0\sigma}(\mathbf{p}) = E_0(\mathbf{p}) + \sigma g \beta_0 B \equiv E_0(\mathbf{p}) + \Delta E_0, \quad (12)$$

where $E_0(\mathbf{p})$ does not depend on the electron spin, g is the electron Landé factor, and $\beta_0 = e\hbar/2m_0c$ is the Bohr magneton (m_0 is the free electron mass). The nonequilibrium correction to the electron distribution function satisfies the equation [7]

$$\delta\rho(\mathbf{p}, \mathbf{s}) = \overline{\delta\rho}(\mathbf{p}, \mathbf{s}) + \frac{\partial f_{\mathbf{p}\sigma}}{\partial E_{\mathbf{p}\sigma}} \sum_{\mathbf{p}', \sigma'} F(\mathbf{p}, \mathbf{s}; \mathbf{p}', \mathbf{s}') \delta\rho(\mathbf{p}', \mathbf{s}'), \quad (13)$$

where $\overline{\delta\rho}(\mathbf{p}, \mathbf{s})$ describes the deviation of the electron liquid from the state of local equilibrium. When the deviation arises due to the effect of the applied magnetic field $\overline{\delta\rho} = -(\partial f_{\mathbf{p}\sigma}/\partial E_{\mathbf{p}\sigma}) g \beta_0 B$. Substituting equation (11) into (13) and using the result in equation (1) we get

$$\Delta E = \Delta E_0 - b^* \sigma g \beta_0 B \equiv \frac{\sigma g \beta_0 B}{1 + b_0}, \quad (14)$$

where $b^* = b_0/(1 + b_0)$, and b_0 is a dimensionless parameter describing FL interactions of the conduction electrons, namely $b_0 = -v_0(0)\psi_0$, where $v_0(0)$ is the density of states of noninteracting conduction electrons on the Fermi surface in the absence of the magnetic field. This is nothing but the standard Stoner renormalization of the paramagnetic susceptibility. Note that here ψ_0 plays the role of the Stoner parameter $I = \langle \delta^2 E_{xc} / \delta\rho_\uparrow \delta\rho_\downarrow \rangle$ in the density functional theory, or of the contact Coulomb interaction in the many-body theory.

The Luttinger theorem dictates the Fermi surface volume. Therefore, the radius and the cross-sectional areas of the Fermi sphere associated with an isotropic Fermi liquid remain unchanged due to quasiparticle interactions. In realistic metals whose conduction electrons form anisotropic Fermi liquids one may expect some minor changes in the FS geometry to appear. Such effects could be considered elsewhere. In the present work we neglect them. So, in further consideration we assume that FL interactions do not affect the FS geometry. Then the cross-sectional areas of the Fermi surface $A(p_z)$ cut out by the planes perpendicular to the magnetic field \mathbf{B} do not change when electron-electron interactions are accounted for. However, the cyclotron masses of conduction electrons undergo renormalization due to the electron-electron interactions. The cyclotron mass is defined as

$$m_\perp = \frac{1}{2\pi} \frac{\partial A}{\partial E} \Big|_{E=\mu} \equiv \oint \frac{dl}{v_\perp}. \quad (15)$$

Here, $dl = \sqrt{dp_x^2 + dp_y^2}$ is the element of length along the cyclotron orbit in the quasimomentum space, $v_\perp = \sqrt{v_x^2 + v_y^2}$, $v_\alpha = \partial E / \partial p_\alpha$ ($\alpha = x, y$), and μ is the chemical potential of conduction electrons.

Substituting equation (11) into (8) we get $v_\perp = v_{\perp 0} / (1 + a_1)$ where $v_{\perp 0} = \sqrt{v_{x0}^2 + v_{y0}^2}$, and a_1 is related to the FL parameter φ_{11} as follows:

$$-v_0(0)p_0^2\varphi_{11}/3 = a_1, \quad (16)$$

where p_0 is the maximum value of the longitudinal component of quasimomentum. So we get

$$m_\perp = m_{\perp 0}(1 + a_1), \quad (17)$$

$m_{\perp 0}$ being the cyclotron mass of noninteracting quasiparticles. In the case of an isotropic electron system the cyclotron mass $m_{\perp 0}$ coincides with the crystalline effective mass m^* . Therefore, our result agrees with the standard isotropic FL theory.

Other quantities, such as the chemical potential of conduction electrons and their compressibility, may experience different renormalizations, as well. The latter, for instance, is renormalized by a factor $1/(1 + a_0) = 1/[1 - v_0(0)\varphi_0]$, and the former by the factor $(1 + a_0)$ [7]. So, the renormalized density of states $\nu(0)$ appears in the expressions for the electron compressibility and the velocity of sound in metals.

The model of the extremely short range (contact) Coulomb interaction between quasiparticles is often employed, while applying the many-body theoretical approach to study the de Haas–van Alphen effect (see e.g. [6]). Within the phenomenological FL theory this model results in the approximation of the functions $\varphi(\mathbf{p}, \mathbf{p}')$ and $\psi(\mathbf{p}, \mathbf{p}')$ by constants φ_0 and ψ_0 , respectively. Such approximation enables us to get the Stoner renormalization of the paramagnetic susceptibility, and electron compressibility as shown above. However, it misses Fermi-liquid effects associated with the subsequent FL coefficients included in equations (9)–(11), which could be significant in renormalizations of other parameters characterizing the charge carriers such as their cyclotron masses.

3. Quantum oscillations of the longitudinal velocity of charge carriers in Q2D conductors

In further calculations we adopt the commonly used tight-binding approximation for the charge carrier spectrum in a quasi-two-dimensional metal. So, when a quantizing magnetic field is applied, the charge carrier energies may be written in the form

$$E_0(n, p_z, \sigma) = \hbar\omega \left(n + \frac{1}{2} \right) + \sigma\hbar\omega_0 - 2t \cos \left(\pi \frac{p_z}{p_0} \right), \quad (18)$$

where $\hbar\omega_0$ is the spin splitting energy, t is the interlayer transport integral, and $p_0 = \pi\hbar/L$ where L is the interlayer distance. This expression (18) describes single-particle energies of noninteracting quasiparticles. Now, the relation of

matrix elements of renormalized $\mathbf{v}_{\nu\nu'}$ and bare $\mathbf{v}_{0\nu\nu'}$ velocities in accordance with equation (8) takes on the form [9]

$$\mathbf{v}_{\nu\nu'} = \mathbf{v}_{0\nu\nu'} - \sum_{\nu_1\nu_2} \frac{f_{\nu_1} - f_{\nu_2}}{E_{\nu_1} - E_{\nu_2}} F_{\nu\nu'}^{\nu_1\nu_2} \mathbf{v}_{\nu_1\nu_2}. \quad (19)$$

Here, E_ν is the quasiparticle energy including the correction arising due to the FL interactions, and $\nu = \{\alpha, \sigma\}$ is the set of quantum numbers of an electron in the magnetic field. The subset α includes the orbital numbers n, p_z and x_0 (the latter labels the positions of the cyclotron orbit centers). Also, $F_{\nu\nu'}^{\nu_1\nu_2} = \varphi_{\alpha\alpha'}^{\alpha_1\alpha_2} + 4\psi_{\alpha\alpha'}^{\alpha_1\alpha_2}(\mathbf{s}\mathbf{s}_1)$ are the matrix elements of the Fermi-liquid kernel.

For an axially symmetrical FS the off-diagonal matrix elements of the longitudinal velocity vanish and we obtain

$$v_{\nu\nu} = v_{0\nu\nu} - \sum_{\nu_1} \frac{df_{\nu_1}}{dE_{\nu_1}} F_{\nu\nu}^{\nu_1\nu_1} v_{\nu_1\nu_1}. \quad (20)$$

Substituting the expression for the Fermi-liquid kernel into equation (20), we get

$$v_{\nu\nu} = v_{\alpha\alpha} \delta_{\sigma\sigma'} + \sigma v_{\alpha\alpha}^s, \quad (21)$$

where both $v_{\alpha\alpha}$ and $v_{\alpha\alpha}^s$ only depend on p_z , so in the further calculations we will use the notation $v_{\alpha\alpha} \equiv v(p_z)$, $v_{\alpha\alpha}^s \equiv v^s(p_z)$. These matrix elements could be found from the system of equations that results from equations (20) and (21):

$$v(p_z) = \left[v_0(p_z) - \sum_{\alpha_1} \varphi_{\alpha\alpha_1}^{\alpha_1\alpha_1} (v(p_{1z})\Gamma_{\alpha_1\alpha_1} + v^s(p_{1z})\Gamma_{\alpha_1\alpha_1}^s) \right], \quad (22)$$

$$v^s(p_z) = - \sum_{\alpha_1} \psi_{\alpha\alpha_1}^{\alpha_1\alpha_1} (v(p_{1z})\Gamma_{\alpha_1\alpha_1}^s + v^s(p_{1z})\Gamma_{\alpha_1\alpha_1}). \quad (23)$$

Here,

$$\Gamma_{\alpha_1\alpha_1} = \sum_{\sigma_1} \frac{df_{\alpha_1\sigma_1}}{dE_{\alpha_1\sigma_1}}, \quad \Gamma_{\alpha_1\alpha_1}^s = \sum_{\sigma_1} \frac{df_{\alpha_1\sigma_1}}{dE_{\alpha_1\sigma_1}} \sigma_1. \quad (24)$$

The de Haas–van Alphen oscillations are observed in magnetic fields when the Landau level spacing is small compared to the chemical potential of electrons ($\hbar\omega \ll \mu$). Under these conditions we may approximate the Fermi-liquid kernel by its expression in the absence of the magnetic fields (equation (2)). Using the above-described approximation of the Fermi-liquid functions $\varphi(\mathbf{p}, \mathbf{p}')$ $\psi(\mathbf{p}, \mathbf{p}')$, equation (11), we can solve equations (22) and (23). To this end, we need some averages over the Fermi surface, namely

$$R = - \sum_{\alpha} \Gamma_{\alpha\alpha} v_0(p_z) p_z = - \frac{1}{4\pi\hbar\lambda^2} \times \sum_{n,\sigma} \int \frac{df(E_{n,\sigma}(p_z))}{dE_{n,\sigma}(p_z)} v_0(p_z) p_z dp_z. \quad (25)$$

$$R' = - \sum_{\alpha} \Gamma_{\alpha\alpha}^s v_0(p_z) p_z. \quad (26)$$

The Fermi-liquid effects enter the systems (22) and (23) through the averages A, A', B, B' closely related to the Fermi-liquid parameters:

$$A = -\varphi_{10} \sum_{\alpha} \Gamma_{\alpha\alpha} p_z^2, \quad A' = -\varphi_{10} \sum_{\alpha} \Gamma_{\alpha\alpha}^s p_z^2. \quad (27)$$

The expressions for B , B' could be obtained replacing φ_{10} by ψ_{10} in equation (27).

Applying the Poisson summation formula,

$$\sum_{n=0}^{\infty} \varphi(n) = \sum_{r=-\infty}^{\infty} \int_0^{\infty} \exp(2\pi irn) \varphi(n) dn \quad (28)$$

to equation (24), we get

$$R = -\frac{1}{4\pi\hbar\lambda^2} \sum_{\sigma} \int dn \int dp_z \frac{df(E_{n,\sigma}(p_z))}{dE_{n,\sigma}(p_z)} v_0(p_z) p_z \times \left\{ 1 + 2 \operatorname{Re} \sum_{r=1}^{\infty} \exp(2\pi irn) \right\}. \quad (29)$$

So, we see that oscillating terms appear in the expressions for R and other averages over the Fermi surface included in equations (22) and (23). For this reason, an oscillating term occurs in the resulting formula for the renormalized longitudinal velocity $v_{\sigma}(p_z)$. This oscillating term originates from the Fermi-liquid interactions between charge carriers, and it appears only when the FL coefficients φ_{10} and ψ_{10} are taken into account, that is, beyond the contact approximation for the Coulomb interaction.

We get the following results for the oscillating parts of R , R' :

$$\tilde{R} = 2N \left(\frac{B}{F} \right) \Delta, \quad R' = 2N \left(\frac{B}{F} \right) \Delta^s, \quad (30)$$

where N is the electron density, and the functions Δ and Δ^s have the form

$$\Delta = \sum_{r=1}^{\infty} \frac{(-1)^r}{\pi r} D(r) \sin\left(2\pi r \frac{F}{B}\right) \cos\left(\pi r \frac{\omega_0^*}{\omega^*}\right) \times J_0\left(4\pi r \frac{t}{\hbar\omega^*}\right), \quad (31)$$

$$\Delta^s = \sum_{r=1}^{\infty} \frac{(-1)^r}{\pi r} D(r) \cos\left(2\pi r \frac{F}{B}\right) \sin\left(\pi r \frac{\omega_0^*}{\omega^*}\right) \times J_0\left(4\pi r \frac{t}{\hbar\omega^*}\right). \quad (32)$$

Here, $F = cA_0/2\pi\hbar e$, A_0 is the FS cross-sectional area at $p_z = \pm p_0/2$; and the cyclotron quantum $\hbar\omega^*$ and spin-splitting energy $\hbar\omega_0^*$ are renormalized according to equations (14) and (17). The damping factor $D(r)$ describes the effects of the temperature and electron scattering on the magnetic quantum oscillations, and $J_0(x)$ is the Bessel function. The simplest and best known approximation for $D(r)$ equates it to the product $R_T(r)R_{\tau}(r)$, where $R_T(r) = rx/\sinh(rx)$ ($x = 2\pi^2 k_B T/\hbar\omega^*$) is the temperature factor and $R_{\tau}(r) = \exp[-\pi r/\omega^* \tau]$ is the Dingle factor describing the effects of electron scattering characterized by the scattering time τ . The temperature factor appears in equations (31) and (32) as a result of standard calculations repeatedly described in the relevant works starting from the LK paper [4]. The Dingle factor cannot be straightforwardly computed starting from the expressions like (25) and (26). This term is phenomenologically included in equation (31) and (32) in the same way as in the Shenberg's book [1]. Under

the low temperatures required to observe magnetic quantum oscillations, the value of τ is mostly determined by the impurity scattering.

Using the microscopic many-body perturbation theory it was shown that in this case the Dingle term retains its form, and the corresponding relaxation time could be expressed in terms of the electron self-energy part Σ arising due to the presence of impurities, namely $\tau^{-1} = 2 \operatorname{Im} \Sigma/\hbar$. In strong magnetic fields the self-energy Σ gains an oscillating term which describes quantum oscillations of this quantity [23, 26]. So, the scattering time becomes dependent on the magnetic field \mathbf{B} . A thorough analysis carried out in the earlier works of Champel and Mineev [26] and Grigoriev [23] shows that the oscillating correction to the scattering time could be neglected when the FS of a Q2D metal is noticeably warped ($4\pi t > \hbar\omega^*$). In such cases one may treat τ as a phenomenological constant. However, when the FS is very close to a pure cylinder ($4\pi t \ll \hbar\omega^*$) the scattering time oscillations must be taken into consideration in studies of the de Haas-van Alphen effect. These oscillations may bring some changes in both shape and magnitude of the magnetization oscillations but we do not discuss the issue in the present work. In further analysis we assume that $4\pi t > \hbar\omega^*$.

One may notice that the oscillating function Δ has exactly the same form as that describing the magnetization oscillations in Q2D metals when the Fermi-liquid effects are omitted from the consideration (see e.g. [23, 24]). Also, the Fermi-liquid terms included in the expression (27) exhibit oscillations in the strong magnetic field. For instance, applying the Poisson summation formula to the expressions (27) we can convert these expressions to the form $A = \bar{a}_1(1+\delta)$, $A' = \bar{a}_1\delta^s$, where the oscillating functions δ and δ^s are

$$\delta = \sum_{r=1}^{\infty} (-1)^r D(r) \cos\left(2\pi r \frac{F}{B}\right) \cos\left(\pi r \frac{\omega_0^*}{\omega^*}\right) S\left(\frac{4\pi r t}{\hbar\omega^*}\right) - \sum_{r=1}^{\infty} (-1)^r D(r) \sin\left(2\pi r \frac{F}{B}\right) \cos\left(\pi r \frac{\omega_0^*}{\omega^*}\right) \times Q\left(\frac{4\pi r t}{\hbar\omega^*}\right), \quad (33)$$

$$\delta^s = \sum_{r=1}^{\infty} (-1)^r D(r) \sin\left(2\pi r \frac{F}{B}\right) \sin\left(\pi r \frac{\omega_0^*}{\omega^*}\right) S\left(\frac{4\pi r t}{\hbar\omega^*}\right) + \sum_{r=1}^{\infty} (-1)^r D(r) \cos\left(2\pi r \frac{F}{B}\right) \sin\left(\pi r \frac{\omega_0^*}{\omega^*}\right) \times Q\left(\frac{4\pi r t}{\hbar\omega^*}\right). \quad (34)$$

The factors S and Q entering equations (33) and (34) are expressed in the series of the Bessel functions:

$$S(x) = J_0(x) + \frac{3}{2\pi^2} \sum_{m=1}^{\infty} \frac{(-1)^m}{m^2} J_{2m}(x), \quad (35)$$

$$Q(x) = \frac{6}{\pi^2} \sum_{m=0}^{\infty} \frac{(-1)^m}{(2m+1)^2} J_{2m+1}(x). \quad (36)$$

The expressions for B, B' are similar to those for A, A' and we may get to the former by replacing the factor \bar{a}_1 by another constant \bar{b}_1 . The oscillating function δ behaves like the function describing quantum oscillations of the charge carrier density of states (DOS) on the FS of a Q2D metal (see the appendix). As for the parameters \bar{a}_1, \bar{b}_1 we can define $\bar{a}_1 = -v_0(0)p_0^2\varphi_{10}/3$ and \bar{b}_1 is similarly defined, namely $\bar{b}_1 = -v_0(0)p_0^2\psi_{10}/3$. We remark that the parameter \bar{a}_1 differs from a_1 , which enters the expression for the cyclotron mass (see equation (17)). This reflects the anisotropy of electron properties in Q2D conductors.

4. Quantum oscillations in the magnetization

To compute the longitudinal magnetization M_{\parallel} , we start from the standard expression:

$$M_{\parallel}(B, T, \mu) \equiv M_z(B, T, \mu) = - \left(\frac{\partial \Omega}{\partial B} \right)_{T, \mu}. \quad (37)$$

Here, the magnetization depends on the temperature T and on the chemical potential of the charge carriers μ , and \mathbf{H} is the external magnetic field related to the field \mathbf{B} inside the metal as $\mathbf{B} = \mathbf{H} + 4\pi\mathbf{M}$. When the magnetic field is directed along a symmetry axis of a high order we may assume that the fields \mathbf{B} and \mathbf{H} are parallel. One may neglect the difference between \mathbf{B} and \mathbf{H} when the magnetization is weak. Otherwise, the uniform magnetic state becomes unstable, and the Condon diamagnetic domains form, with the alternating signs of the longitudinal magnetization¹. We will discuss this possibility later. Now, we neglect the difference between H and B in equation (37). To incorporate the effects of electron interactions we assume, in the spirit of the FL theory, that the thermodynamic potential Ω has the same form as for noninteracting quasiparticles, but with the quasiparticle energies fully renormalized by their interaction:

$$\Omega = -k_B T \sum_v \ln \left\{ 1 + \exp \left[\frac{\mu - E_v}{k_B T} \right] \right\}. \quad (38)$$

In this expression E_v is the quasiparticle energy including the correction arising due to the FL interactions, and k_B is the Boltzmann's constant.

Accordingly, we rewrite equation (38) as follows:

$$\Omega = - \frac{k_B T}{4\pi^2 \hbar \lambda^2} \sum_{n, \sigma} \int \ln \left\{ 1 + \exp \left[\frac{\mu - E_{n, \sigma}(p_z)}{k_B T} \right] \right\} dp_z, \quad (39)$$

where $\lambda^2 = \hbar c/eB$ is the squared magnetic length. Performing integration by parts, equation (39) becomes

$$\Omega = - \frac{1}{4\pi^2 \hbar \lambda^2} \sum_{n, \sigma} \int f(E_{n, \sigma}(p_z)) v_{\sigma}(p_z) p_z dp_z. \quad (40)$$

Applying the Poisson summation formula, we get

$$\Omega = - \frac{1}{4\pi^2 \hbar^3 \lambda^2} \sum_{\sigma} \int dn \int dp_z f(E_{n, \sigma}(p_z)) v_{\sigma}(p_z) p_z \times \left\{ 1 + 2 \operatorname{Re} \sum_{r=1}^{\infty} \exp[2\pi i r n] \right\}. \quad (41)$$

¹ A review of the current theory of the diamagnetic phase transitions in metals is given by [28]

So we see that the expression for the thermodynamic potential includes two oscillating terms. One originates from the oscillating part of $v_{\sigma}(p_z)$. The second term inside the braces in the equation (41) gives another oscillating contribution.

The effects of temperature and spin splitting on the magnetic oscillations are already accounted for in equation (41). Assuming $4\pi t > \hbar\omega$, we take into account the effect of electron scattering, adding an imaginary part $i\hbar/2\tau$ to the electron energies [1]. After standard manipulations, we obtain the following expression for the oscillating part of the longitudinal magnetization:

$$\Delta M_{\parallel} = -2N\beta \frac{\omega_0^*}{\omega^*} (1 - 3a_1^*) \times \frac{\Delta - 3(a_1^* + b_1^*)\delta + 3b_1^*(\Delta\delta - \Delta^s\delta^s) - 9a_1^*b_1^*(\delta^2 - \delta^s{}^2)}{1 + 3(a_1^* + b_1^*)\delta + 9a_1^*b_1^*(\delta^2 - \delta^s{}^2)}, \quad (42)$$

where $a_1^* = \bar{a}_1/(1 + 3\bar{a}_1)$; $b_1^* = \bar{b}_1/(1 + 3\bar{b}_1)$. This is the main result of the present work. It shows that the Fermi-liquid interactions may bring significant changes in the de Haas-van Alphen oscillations. Below, we analyze these changes. If we may neglect the oscillating corrections proportional to a_1^*, b_1^* , then our result for ΔM_{\parallel} reduces to the usual LK form with some renormalizations arising from the quasiparticle interactions. The cyclotron mass m_{\perp} differs from the bare Fermi-liquid cyclotron mass before the quasiparticle interaction is taken into account (cf. equation (17)), and $\hbar\omega_0^*$ includes the extra factor $(1 + b_0)^{-1}$. Also, the factor $(1 - 3a_1^*)$ modifies the magnetic oscillation magnitudes. As for the oscillation frequencies, they remain unchanged by the FL interactions, as expected.

5. Discussion

Comparing our result (42) with the corresponding result reported by Wasserman and Springfield [6], we see that these results agree with each other. A seeming difference in the expressions for the oscillation frequencies arises due to the fact that in [6] the frequencies are expressed in terms of the chemical potential of electrons μ instead of the cross-sectional areas of the Fermi surface. It is worth reiterating that 'unrenormalized' mass in the FL theory is already renormalized (sometimes strongly) from fully noninteracting (or density-functional-calculated) mass. Again, we remark that the present analysis was carried out assuming noticeable/significant FS warping ($4\pi t > \hbar\omega^*$), so we may neglect the magnetic field dependence of the electron scattering τ , treating the latter as a constant phenomenological parameter. This results in a simple form of the Dingle damping factor $R_{\tau}(r)$ describing the effects of electron impurity scattering.

The LK form of the expression for the longitudinal magnetization is suitable to describe de Haas-van Alphen oscillations in conventional three-dimensional metals within the whole range of temperatures. However, this is not true for quasi-two-dimensional conductors. The Fermi surface of such a conductor is nearly cylindrical in shape, therefore the oscillating term in the denominator of equation (42) significantly increases. The oscillations of the denominator

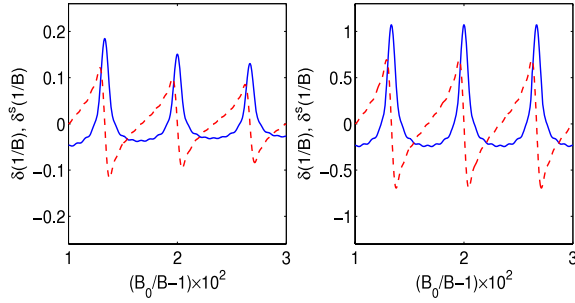


Figure 1. The magnetic field dependences of the functions δ (solid lines) and δ^s (dashed lines). The curves are plotted at $B_0 = 10$ T, $F/B_0 = 300$, $2\pi^2\theta^*/\hbar\omega^* = 0.5$ for $t/\hbar\omega^* = 2$ (left panel) and $t/\hbar\omega^* = 0.3$ (right panel).

of equation (42) occur due to the functions δ and δ^s . These functions are presented in figure 1, and we see that at low temperatures and weak scattering $\ln(\hbar\omega^*/k_B T^*) > t/\hbar\omega^*$ ($T^* = T + T_D$, $T_D = \hbar/2\pi k_B \tau$ is the Dingle temperature) the peak values may be of the order of unity, especially for a rather weakly warped FS ($t/\hbar\omega^* \sim 0.1-0.5$). So, quantum oscillations in the magnetization in the electron Fermi liquid in quasi-two-dimensional metals may have more complicated structure than those in the electron gas described by the LK formula [4]. The effect of the Fermi-liquid interactions on these oscillations depends on the values of the Fermi-liquid parameters a_1^* , b_1^* and on the damping factor $D(r) = R_T(r)R_\tau(r)$ included in the expressions for the oscillating functions. The FS shape determined by the ratio $t/\hbar\omega$ is important as well.

The most favorable conditions for the changes in the magnetization oscillations to be revealed occur when the oscillating terms in the denominator of equation (42) may take on values of the order of unity at the peaks of oscillations. We may estimate the peak values δ_m and δ_m^s of the functions included in the above denominator using the Euler-Macloren formula. The estimations depend on the shape of the FS of the Q2D conductor. When the FS is significantly crimped ($t \gg \hbar\omega$) we obtain $\delta_m, \delta_m^s \sim (\hbar\omega/t)^{1/2} (k_B T^*)^{-1/2}$. So, we may expect the Fermi-liquid interaction to be distinctly manifested in the magnetization oscillations when $|a_1^*|(\hbar\omega/t)^{1/2} (k_B T^*)^{-1/2} \sim 1$ or $|b_1^*|(\hbar\omega/t)^{1/2} (k_B T^*)^{-1/2} \sim 1$ or both. In all probability the Fermi-liquid parameters are small in magnitude ($|a_1^*|, |b_1^*| \ll 1$). Nevertheless, the changes in the de Haas-van Alphen oscillations arising due to the Fermi-liquid effects may occur at $k_B T^* \ll 1$. It is worthwhile to remark that, due to the character of the electron spectra, the Q2D conductors provide better opportunities for observations of the Fermi-liquid effects in the de Haas-van Alphen oscillations than conventional 3D metals. In the latter the peak values of the oscillating functions δ, δ^s have the order $(\hbar\omega/\mu)^{1/2} (k_B T^*)^{-1/2}$. Typical values of the transfer integral t are much smaller than those of the chemical potential μ ; therefore, significantly smaller values of $k_B T^*$ and/or greater values of the parameters a_1^*, b_1^* are required for the Fermi-liquid effects to be revealed in 3D metals.

Due to the special character of the electron spectra in the Q2D metals, the variations in the magnetization oscillations

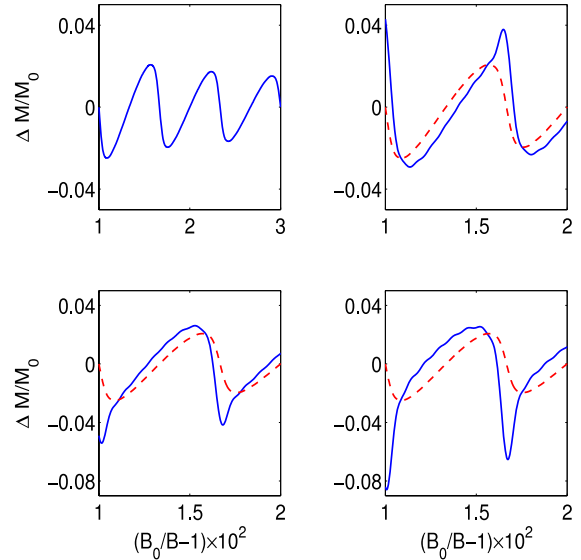


Figure 2. The effect of the Fermi-liquid interactions on the de Haas-van Alphen oscillations in a Q2D metal at $t/\hbar\omega^* = 2$. The curves are plotted using equation (42), $M_0 = 2N\beta$. Calculations are carried out for $a_1^* = b_1^* = 0$ (top left panel), $a_1^* = b_1^* = 0.02$ (top right panel), $a_1^* = b_1^* = -0.02, -0.04$ (bottom left and right panels, respectively). The remaining parameters are the same as used in figure 1. The dashed lines in the top right panel and in the bottom panels represent oscillations in the system of noninteracting quasiparticles.

may be noticeable at reasonably small values of the Fermi-liquid constants. In figure 2 we compare the oscillations arising in a gas of the charge carriers (top left panel) with those influenced by the Fermi-liquid interactions between them. All curves included in this figure are plotted within the limit $t > \hbar\omega$. We see that both magnitude and shape of the oscillations noticeably vary due to the Fermi-liquid effects. When $t/\hbar\omega^* \sim 0.1-0.5$ the FS shape is closer to a perfect unwarped cylinder; the magnetization oscillations accept the well known sawtoothed shape, shown in figure 3. Again, when the Fermi-liquid interaction produced terms are included in the expression for ΔM , this brings some changes in the magnitude and shape of the oscillations. These changes are more significant when $(a_1^* + b_1^*) < 0$.

The most important manifestation of the Fermi-liquid effects occurs in very clean conductors at low temperatures when T^* is reduced so much that $(a_1^* + b_1^*)\delta_m$ is greater than unity. Then the denominator of equation (42) becomes zero at some points near the peaks of the DOS oscillations provided that $(a_1^* + b_1^*) < 0$. This is illustrated in figure 4. Correspondingly, ΔM diverges at these points, which indicates the magnetic instability of the system.

This means that the condition for the uniform magnetization of the electron liquid is violated near the oscillation maxima, and diamagnetic domains could emerge. It is known that both crystal anisotropy and demagnetization effects originating from the shape of the metal sample could modify the relation between \mathbf{B} and \mathbf{H} and cause magnetic instability, which results in the occurrence of the diamagnetic domains [28] (see footnote 1). Our result demonstrates that the interactions of con-

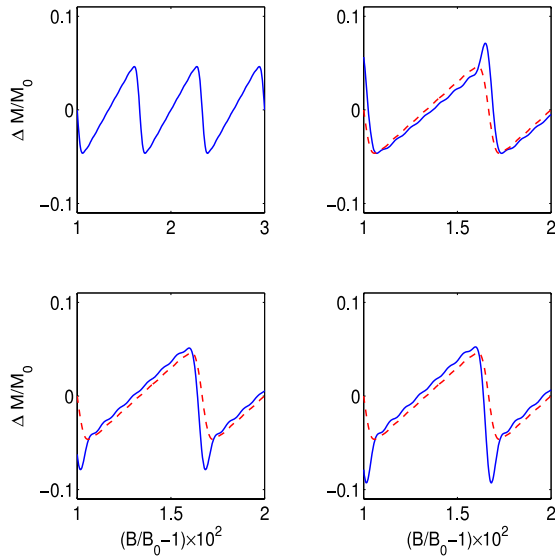


Figure 3. The effect of the Fermi-liquid interactions on the de Haas–van Alphen oscillations in a Q2D metal at $t/\hbar\omega^* = 0.3$. The curves are plotted using equation (42) at $a_1^* = b_1^* = 0$ (top left panel), $a_1^* = b_1^* = 0.02$ (top right panel), $a_1^* = b_1^* = -0.02$ (bottom left panel), and $a_1^* = b_1^* = -0.04$ (bottom right panel). The remaining parameters are the same as in figure 1. Dashed lines represent the oscillations in the gas of charge carriers.

ducting electrons also may play an important role in magnetic phase transitions. In principle, such magnetic instabilities may appear in 3D metals as well, which was shown earlier, analyzing quantum oscillations in the longitudinal magnetic susceptibility of the isotropic electron liquid (see [18, 29]). However, we may hardly expect these transitions to appear in conventional metals, for the requirements on the temperature and intensity of scattering processes are very strict. Estimations made in the earlier works [20, 29] show that the temperature (including the Dingle correction) must be about 10 mK or less for these diamagnetic phase transitions to emerge in conventional metals. In contrast, the special (nearly cylindrical) shape of the FS in Q2D conductors gives grounds to expect the above transitions to appear in realistic experiments.

To summarize, in the present work we theoretically analyzed possible manifestations of the FL interactions (that is, residual interactions of excited quasiparticles) in the de Haas–van Alphen oscillations in Q2D conductors. The same approach can be easily applied for a metal with a crystalline lattice of arbitrary symmetry, using the appropriate basis for expanding the FL functions. So, the phenomenological Fermi-liquid theory becomes more realistic and suitable to analyze effects of electron interactions in actual metals.

We showed that the residual quasiparticle interactions affect all damping factors inserted in the LK formula through the renormalization of the cyclotron mass. The spin splitting is renormalized as well, in a manner similar to the so-called Stoner enhancement. The frequency of the oscillations remains unchanged, for it is determined with the main geometrical characteristics of the Fermi surface, which probably are not affected by electron–electron interactions. However, the shape and magnitude of the oscillations are affected due

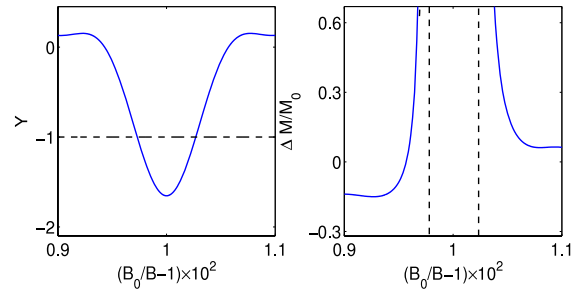


Figure 4. The plot of the function $Y = (a_1^* + b_1^*)\delta + a_1^*b_1^*(\delta^2 - \delta^{s^2})$ near the peak of the DOS quantum oscillations at $t/\hbar\omega^* = 0.3$, which illustrates that the denominator in equation (42) may become zero in the vicinities of these peaks (left panel). The divergencies in the oscillating part of magnetization described by equation (42) indicate the magnetic instability caused by the Fermi-liquid effects (right panel). The curves are plotted assuming $a_1^* = b_1^* = -0.04$. The remaining parameters have the same values as used in figure 1.

to the FL effects, and their changes may be noticeable. Also, the obtained results indicate that (under the relevant conditions) the electron interactions may break down the magnetic stability of the material, creating an opportunity for the diamagnetic phase transition. The discussed effects may be available for observations in realistic experiments, bringing extra information concerning electronic properties of quasi-two-dimensional metals.

Finally, we want to emphasize once again that the renormalizations, most importantly mass renormalization, are *in addition* to what is conventionally called ‘mass renormalization’, namely, renormalization of the specific heat coefficient compared to band structure calculations. It is usually implicitly assumed that the weighted average of the de Haas–van Alphen mass renormalization is exactly equal to the specific heat renormalization, i.e., the FL effects are small. In many cases this is a good approximation, but one can never exclude a possibility that in some materials these two masses may be different, namely, the de Haas–van Alphen mass may be larger. A curious example when one would have needed to exercise caution, but did not, is given by [30], where quantum oscillations in a highly unconventional metal, Na_xCoO_2 , were measured, and it was taken for granted that the large mass renormalization found in the experiment should be fully accounted for in specific heat. Based on this assumption, a natural and straightforward interpretation of the data was abandoned and a counterintuitive explanation, requiring some unverified assumptions, was accepted. It is possible that the results reported in reference [30] give a case where additional mass renormalization discussed in this paper is significant. Hopefully, at some point we will see a careful and accurate experimental study on various materials that would compare the de Haas–van Alphen masses with the thermodynamic masses and give us a quantitative answer on how different may the two be in real life.

Acknowledgments

The author thanks G Kotliar and I Mazin for helpful discussions, and G M Zimbovsky for help with the manuscript.

This work was supported by DoD grant W911NF-06-1-0519 and NSF-DMR-PREM 0353730.

Appendix

Here, we analyze the expressions for the oscillating functions δ , δ^s within the limits of significant ($t \gg \hbar\omega$) FS warping. We may use the standard asymptotics for the Bessel functions, at $x \gg 1$, namely

$$J_k(x) \approx \sqrt{\frac{2}{\pi x}} \cos \left[x - \frac{\pi k}{2} - \frac{\pi}{4} \right]. \quad (43)$$

Substituting these approximation into equations (34) and (35) we obtain

$$S(x) = \sqrt{\frac{2}{\pi x}} \cos \left[x - \frac{\pi}{4} \right] \left\{ 1 + \frac{3}{\pi^2} \sum_{m=1}^{\infty} \frac{1}{m^2} \right\}, \quad (44)$$

$$Q(x) = \frac{6}{\pi^2} \sqrt{\frac{2}{\pi x}} \sin \left[x - \frac{\pi}{4} \right] \sum_{m=0}^{\infty} \frac{1}{(2m+1)^2}, \quad (45)$$

where

$$\sum_{m=1}^{\infty} \frac{1}{m^2} = \frac{\pi^2}{6}, \quad \sum_{m=0}^{\infty} \frac{1}{(2m+1)^2} = \frac{\pi^2}{8}. \quad (46)$$

So, we have:

$$S(x) = \frac{5}{4} \sqrt{\frac{2}{\pi x}} \cos \left[x - \frac{\pi}{4} \right], \quad (47)$$

$$Q(x) = \frac{3}{4} \sqrt{\frac{2}{\pi x}} \sin \left[x - \frac{\pi}{4} \right]. \quad (48)$$

Using these results we may write the following expressions for δ , δ^s at $t \gg \hbar\omega$:

$$\begin{aligned} \delta &= \frac{5}{4} \left(\frac{\hbar\omega^*}{2\pi^2 t} \right)^{1/2} \sum_{r=1}^{\infty} \frac{(-1)^r}{\sqrt{r}} D(r) \cos \left[2\pi r \frac{F}{B} \right] \\ &\times \cos \left[\frac{4\pi r t}{\hbar\omega^*} - \frac{\pi}{4} \right] \cos \left[\pi r \frac{\omega_0^*}{\omega^*} \right] \\ &- \frac{3}{4} \left(\frac{\hbar\omega^*}{2\pi^2 t} \right)^{1/2} \sum_{r=1}^{\infty} \frac{(-1)^r}{\sqrt{r}} D(r) \sin \left[2\pi r \frac{F}{B} \right] \\ &\times \sin \left[\frac{4\pi r t}{\hbar\omega^*} - \frac{\pi}{4} \right] \sin \left[\pi r \frac{\omega_0^*}{\omega^*} \right]. \end{aligned} \quad (49)$$

Or

$$\begin{aligned} \delta &= \left(\frac{\hbar\omega^*}{2\pi^2 t} \right)^{1/2} \sum_{r=1}^{\infty} \frac{(-1)^r}{\sqrt{r}} D(r) \cos \left[\pi r \frac{\omega_0^*}{\omega^*} \right] \\ &\times \left\{ \cos \left[2\pi r \frac{F_{\max}}{B} - \frac{\pi}{4} \right] + \frac{1}{4} \cos \left[2\pi r \frac{F_{\min}}{B} + \frac{\pi}{4} \right] \right\}. \end{aligned} \quad (50)$$

Likewise, we obtain for δ^s

$$\begin{aligned} \delta &= \left(\frac{\hbar\omega^*}{2\pi^2 t} \right)^{1/2} \sum_{r=1}^{\infty} \frac{(-1)^r}{\sqrt{r}} D(r) \cos \left[\pi r \frac{\omega_0^*}{\omega^*} \right] \\ &\times \left\{ \sin \left[2\pi r \frac{F_{\max}}{B} - \frac{\pi}{4} \right] + \frac{1}{4} \sin \left[2\pi r \frac{F_{\min}}{B} + \frac{\pi}{4} \right] \right\}. \end{aligned} \quad (51)$$

Here, F_{\max} and F_{\min} correspond to the maximum and minimum cross-sectional areas of the FS, respectively.

References

- [1] Shoenberg D 1984 *Magnetic Oscillations in Metals* (New York: Cambridge University Press)
- [2] Wosnitzer J 1996 *Fermi Surface of Low-Dimensional Organic Metals and Superconductors* (Berlin: Springer)
- [3] Singleton J 2000 *Rep. Prog. Phys.* **63** 1111
- [4] Lifshitz I M and Kosevich A M 1956 *JETP* **2** 636
- [5] Luttinger J M 1961 *Phys. Rev.* **121** 1251
- [6] See Wasserman A and Springfield M 1996 *Adv. Phys.* **45** 471 and references therein
- [7] Pines D and Nozières P 1966 *Theory of Quantum Liquids* (Boston, MA: Benjamin)
- [8] Abrikosov A A 1988 *Foundations of the Theory of Metals* (Amsterdam: North-Holland)
- [9] Zimbovskaya N A 2001 *Local Geometry of Fermi Surface and High-Frequency Phenomena in Metals* (New York: Springer)
- [10] Mazin I I and Cohen R E 1997 *Ferroelectrics* **164** 263
- [11] Platzman P M and Wolff P A 1973 *Waves and Interactions in Solid State Plasma* (New York: Academic)
- [12] Platzman P M and Walsh P A 1967 *Phys. Rev. Lett.* **19** 519
- [13] Platzman P M, Walsh P A and Foo E N 1968 *Phys. Rev.* **172** 689
- [14] Zyryanov P S, Okulov V I and Silin V P 1968 *JETP Lett.* **8** 432
Zyryanov P S, Okulov V I and Silin V P 1969 *JETP Lett.* **9** 283
- [15] Zimbovskaya N A 1995 *J. Low. Temp. Phys.* **21** 217
- [16] Zimbovskaya N A 2007 *Phys. Rev. B* **76** 075104
- [17] Kirichenko O V, Peschansky V G and Stepanenko D I 2005 *Phys. Rev. B* **71** 045304
- [18] Bagaev V N, Okulov V I and Pamyatnykh E A 1978 *JETP Lett.* **27** 144
- [19] Testardi L R and Condon J H 1970 *Phys. Rev. B* **1** 3928
- [20] Zimbovskaya N A 2005 *Phys. Rev. B* **71** 024109
- [21] Harrison N, Bogaerts R, Reinders P H P, Singleton J, Blundell S J and Herlach F 1996 *Phys. Rev. B* **54** 9977
- [22] Champel T 2001 *Phys. Rev. B* **64** 054407
- [23] Grigoriev P D 2003 *Phys. Rev. B* **67** 144401
- [24] Gvozdkov V M, Jansen A G M, Pesin D A, Vagner I D and Wyder P 2003 *Phys. Rev. B* **68** 155107
- [25] Carrington A, Fletcher J D and Harima T 2005 *Phys. Rev. B* **71** 174505
- [26] Champel T and Mineev V P 2002 *Phys. Rev. B* **66** 19511
- [27] Allen P B 1976 *Phys. Rev. B* **13** 1416
- [28] Gordon A, Vagner I D and Wyder P 2003 *Adv. Phys.* **52** 385
Yelland E A, Cooper J R, Carrington A, Hussey N E, Meeson P J, Lee S, Yamamoto A and Tajima S 2002 *Phys. Rev. Lett.* **88** 217002
- [29] Bagaev V N, Okulov V I and Pamyatnykh E A 1978 *Sov. J. Low Temp. Phys.* **4** 316
- [30] Bourgeois A, Aligia A A, Kroll T and Nunez-Regueiro M D 2007 *Phys. Rev. B* **75** 174518